Assessing the weathering of basaltic aggregates using image texture analysis

Edson Aparecido Martins Filho, Lilian Tais de Gouveia, Luciano Jose Senger[1]

[1]Universidade Estadual de Ponta Grossa (UEPG) – Ponta Grossa – PR – Brasil

edson.martins94@gmail.com, ltgouveia@uepg.br, ljsenger@uepg.br

Abstract. *Mineral aggregates are the most mined materials in the world. Aggregates are a component of composite materials such as asphalt concrete, used mainly in highway´s paving. The importance of aggregate is because it serves as reinforcement to add strength to the overall composite material. Aggregates should be obtained from non-weathered rocks. Aggregates from weathered rocks commonly present low resistance to abrasion and compression, especially under conditions of frequently repeated vehicle's load, such as on highways. This paper presents an evaluation of image texture analysis when applied to detect the presence of weathering in aggregates. An evaluation of the texture analysis using histograms, entropy, local binary patterns and local phase quantization as descriptors aiming to identify weathering in basaltic aggregates is presented. These texture descriptors and the Naive Bayes, IBK, J48 and Multilayer Perceptron machine learning algorithms were used to detect the presence of weathering in aggregates. The results obtained indicated that red channel stands out as descriptor to differentiate weathered from non-weathered aggregates with an average error around 4%.*

Keywords: image processing, texture analysis, machine learning.

1. Introduction

Mineral aggregates are used as the main constituent of many materials used in engineering works, including Portland cement concrete, asphalt concrete, road bases, railroad ballast, filtration systems and soil stabilization. Consequently, millions of tons of mineral aggregates are extracted and consumed by the industry every year [1].

Adequate aggregates must be healthy, with no signal of weathering. Weathered aggregates commonly present low resistance to abrasion and compression, especially under conditions of frequently repeated vehicle's load, such as on highways. Premature defects that occur in works can often be related to the use of non-detected weathered aggregates.

The weathering of aggregates occurs when the rocks are exposed to environmental conditions different from those where they were formed, in contact with new physical and chemical processes, which differ greatly from the original conditions. Physical weathering creates micro and macro fractures in the rocks that will allow the infiltration of aqueous solutions and the action of living micro-organisms, thus initiating a series of chemical reactions that vary depending on the environmental conditions and the mineralogical composition of the rocks [2].

When aggregates are subjected to weathering, they start to show variation in their color, due to the decomposition of the rock-forming minerals. Figure 1 illustrates the variation in color between two aggregates from same origin (diabase). The first one is weathered and the second one preserves its natural colors. However, not all weathered aggregate particles present so accentuated variations in coloring. Generally, what happens is that a fraction of particles in the aggregate start to show levels of weathering, and this is often not detected by the quarries. The weathering occurs gradually, and the minerals present in the aggregates take a relatively long time to undergo changes, which may vary depending on the type of minerals from the rock and local climatic conditions, or

weathering conditions. Thus, the aggregates can present themselves in different stages of weathering, or degrees of weathering.

Figure 1: Texture of weathered (left) and non-weathered (right) aggregates samples.

This paper presents an evaluation of texture analysis when applied to detect the present the weathering in aggregates. Texture analysis techniques are often used for classification purposes, for example, identification of cancer cells, plant diseases, detection of defects in metals, etc. However, specifically for detecting changes in rocks, where differentiation of the physical characteristics of the material is observed as the change develops, there is a need to investigate these techniques. During the development of the alteration in the rocks, some phenomena are observed including erosion or dissolution of the material, increased porosity and increase in the degree of cracking. Therefore, perhaps texture analysis techniques can identify these changes, if they are sensitive enough to identify these differences in the texture of the materials.

2. Related Work

There are methods of detecting weathering in aggregates. Maia [3] presents a comprehensive review of such methods and quality indexes used to assess the alteration of rocks. The survey includes methods for analyzing apparent porosity, petrographic and water absorption analysis, fine particle size, voids index, specific surface, ultrasound propagation speed, sanity of samples to sodium or magnesium sulfate, chemical analysis, Los Angeles abrasion, leaching, Treton impact and petrographic texture analysis. In Brazil, the Los Angeles abrasion and the soundness tests are frequently adopted to assess soundness of mineral rocks.

The Los Angeles abrasion test reproduces the impact on the sample by dropping the steel balls on the aggregates and dropping the aggregates themselves, on top of each other, and simulates wear by rubbing the aggregates together and with the walls of the drum while rotating at a speed of 30 to 33 rpm, until the number of 500 revolutions is completed. Then, the material is removed from the drum, sieved and weighed. The test result is the percentage of material loss due to mechanical degradation. In Brazil, DNER (Brazil´s National Highway Authority) accepts values for Abrasion Los Angeles ≤ 50% and DER-PR ≤ 45%.

The soundness test determines on aggregate's resistance to disintegration by weathering and provides an indication of durability in the face of time. This test involves cycles of submerging the aggregate in sodium or magnesium sulfate solution and drying. During the dry stage, salts accumulate in aggregate voids. In re-immersion, the salt crystals hydrate and grow in the pores of the aggregates, exerting internal expansion forces that cause the disintegration of some particles. The test result is the percentage of material loss over a series of screens for five freeze-thaw cycles. The maximum loss values vary between 10 to 20% for 5 cycles. The DER-PR admits a maximum loss of 12%.

The analysis of aggregate texture is particularly interesting because it assesses the visible effects of the weathering process. These effects are related to the color appearance of the aggregates, such as discoloration, rust spots, superficial darkening, that is, these altered materials start to present on their surface colors different from those consistent with their original mineralogical condition [4].

Image analysis methods have been suggested to evaluate aggregates. A review of these methods was presented by [5]. Among the imaging methods that have been used for aggregate analysis, approaches based on the Hough Transform [6]; fractal morphology to assess the angularity of the fine aggregate [7]; gray-scale Wavelet decomposition for analysis of surface texture using binary images to characterize the shape of the aggregate [8]; Fourier analysis applied to the aggregate particle profiles to determine the general and angularity of these elements [9]; and a multiscale curvature method for analyzing the shape and angularity of the coarse and fine aggregate [10], an entropy method to determine the degree of change in basalt aggregates [11].

3. Background

Texture analysis can be used to identify objects or regions of interest in digital images. Texture is a characteristic related to the physical properties of an object's surface. Thus, the texture describes the pattern of gray or color variation of a given region of interest and provides information about the spatial distribution of an object's shade variations. The texture describes the visual impression of roughness or smoothness of a given surface. The Figure 2 illustrates some examples of textures.

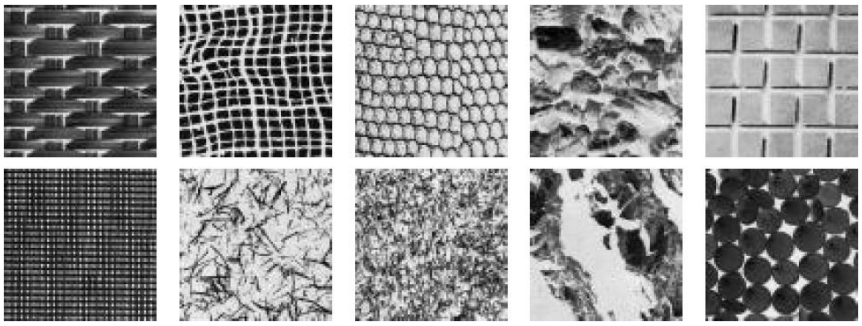

Figure 2: Examples of textures in digital images

The main approaches to the analysis of textures are the statistical and the structural. In the statistical approaches, the distribution of gray levels and the relationship of these values through statistical measures are used. The structural approaches represent texture by well defined primitives and a hierarchy of spatial arrangements of those primitives. In the statistical approaches, texture analysis is mainly conducted through the use of histograms.

In image processing, a histogram is used to account for the percentage of pixels in the image, considering shades of gray (monochrome image) or each RGB channel in the image. The histogram imaging technique associates an h (n) value for each gray (or color) level of the image. The h (n) values correspond to the number of times, or frequency, that shades of gray or color occur in the image. The pixel's intensity information can be obtained in grayscale or in each of the image's RGB channels. Thus, for each original image, in color, you can obtain three histograms, one for each RGB component, in addition to the gray level histogram .

As statistical approach method, the entropy measure can be applied for texture analysis [11]. The entropy developed by Claude Shannon is a probabilistic process that measures the amount of information that is associated with a channel, that is, the number of bits needed to

describe a random variable. The higher the entropy value of an image, the more irregular and atypical (non-standard) the analyzed image is. Therefore, the higher the entropy value, the more information will be associated with the channel. The concept of entropy applied to image analysis defines that the generation of information can be modeled as a probabilistic process. An image is considered as a random process where p(i) is the probability of a pixel i in the range 0 and N. Therefore, the entropy value for an image can be obtained through the following equation:

$$p(i) = \frac{h(i)}{P * Q}$$

In an image where all pixels have the same hue, entropy is equal to zero. The entropy calculation does not take into account the spatial arrangement of pixel tones, that is, the entropy value is not affected by image rotating [11].

Local Binary Patterns (LBP) is a representative detector for structural texture analysing. This detector has been used in several areas, for instance in facial recognition applications [12,13] and wood species recognition [14]. The LBP detector produces grayscale texture descriptors, whose values are calculated using a binary value assigned to each pixel in the image, forming a linear neighborhood of radius R around a central pixel. Although an 8-bit neighborhood is commonly used, there are variants of the algorithm, mainly in relation to the number of pixels (radius) to be adopted. Another variation is the use separately or combined of the RGB channels of the image.

The LBP operator is denoted by $LBP_{P,R}$ and defined as:

$$\mathrm{LBP}_{\mathrm{P,R}} = \sum_{\mathrm{i}=1}^{\mathrm{P}-1} 2^{\mathrm{i}} \mathrm{S}(\mathrm{p_i} - \mathrm{p_c})$$

$$S(x) = \begin{cases} 1, & if\ x \geq 0 \\ 0, & otherwise \end{cases}$$

where P is the total number of pixels in the neighborhood, R is the radius, $\mathrm{p_i}$ describes a surrounding pixel *i* and pc is the central pixel. Common values for the neighborhood size and radius are: (8, 1), (16, 2), and (8, 2) [15]. The Figure 3 illustrates the process of obtaining an $LBP_{P,R}$ descriptor in which the descriptor value of 10000111 is obtained for an arbitrary pixel, considering that the encoding starts from the upper left neighbor. Each descriptor represents a texture feature.

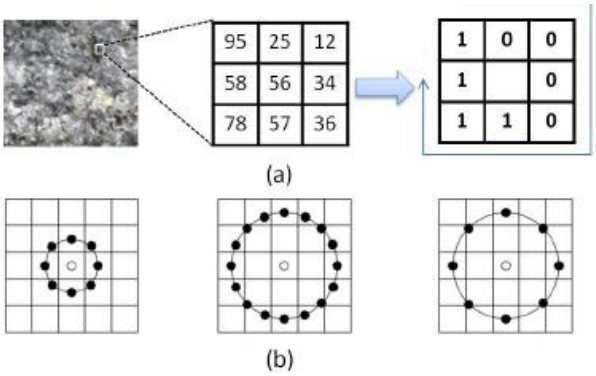

Figure 3: Example of an LBP detector from a gray level image (a) and its distinct radius and neighbor values: (8, 1), (16, 2), e (8, 2) (Adapted from [15]).

The Figure 4 depicts examples of binary matrices (descriptors) that can be obtained for an image, considering a neighborhood of size (8,1). Histogramas are used to group the $LBP_{P,R}$

descriptors. Considering a neighborhood (8,1), it is possible to obtain 256 distinct descriptors for an image, that is, the histogram represents 256 distinct patterns. By this way, an image texture are represented by its LBP histogram.

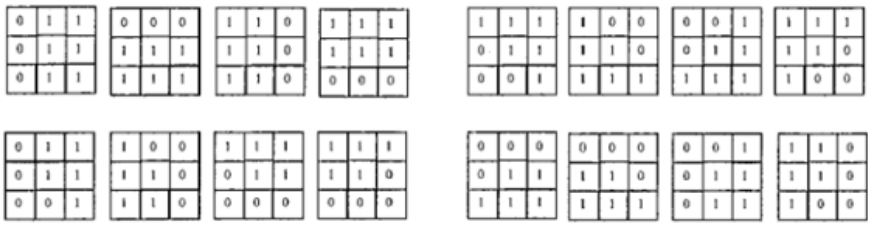

Figure 4: LBPp,r binary matrices.

Since the $LBP_{p,r}$ detector is computed using the pixel neighborhood gray levels, its value depends on the first pixel choosen to start the encoding. This issue was studied by [16] who introduced two variations in the traditional LBP method: the LBP_{ri} (*rotation invariant*) detector, and the LBP_{riu} (*rotation invariant uniform*) detector. When using the LBP_{ri} detector, the obtained descriptor is rotated (bitshifting) P (P = neighborhood size) circularly to the right, so that for each descriptor P a set of derived descriptors are obtained. Afterwards, the derived descriptor with the lowest numerical value is chosen to represent the feature class. Considering such an operation and a neighborhood size (8,1), it is possible to reduce the number of possible different descriptors from 256 to 36.

The LBP_{riu} can be used to reduce the length of the feature vector by implementing a simple rotation invariant descriptor. The motivation is the fact that some binary patterns occur more commonly in texture images than others. A local binary pattern is called uniform if its value contains at most two 0-1 or 1-0 transitions. Using uniform patterns, the length of the feature vector is reduced from 256 to 59.

Another variant of the $LBP_{p,r}$ algorithm is the Local Phase Quantization (LPQ) algorithm, which has demonstrated good performance in specific texture analysis applications, in which there is movement or lack of focus in the acquisition of images [17]. LPQ is a method of obtaining descriptors in scenarios where there is degradation in the images obtained. The method is not affected by factors that can degrade the image, for example, movement and lack of focus on the camera. The LPQ descriptor is computed by means of a Short-Term Fourier Transform [18].

Machine learning where used to evaluate the descriptors and to build classification models. Among the learning algorithms, in this paper the IBk, Naive Bayes, J48 and Multi Layer Perceptron algorithms were evaluated [20]. Such algorithms are often adopted for the purpose of classification with recognized success.

4. Material and Methods

Images of basalt aggregates were obtained, with 202 particles of weathered basalt aggregates and 251 particles of non-weathered aggregates. A high definition scanner (4800 dpi) was used to acquire the images. The aggregate particles were placed on the scanner, supporting each particle under its largest axis, that is, the axis of greatest stability. The images were obtained with a resolution of 300 dpi in a dark environment, thus avoiding interference from light sources. It was observed that, under these conditions, the edges of the aggregate were well defined. An example of image scanning result is presented in Figure 5.

After acquiring the images, they were pre-processed to eliminate noising. The next step was the detection of the contour of the aggregates, in order to obtain the information only from the foreground of the aggregates, disregarding the background image. Then, image descriptors were

computed, obtaining the gray-colored histograms and histograms for each RGB color channel, as well as the LBP histograms and entropy values. Image processing was carried out using a computer program developed using the C language and the OpenCV library [19].

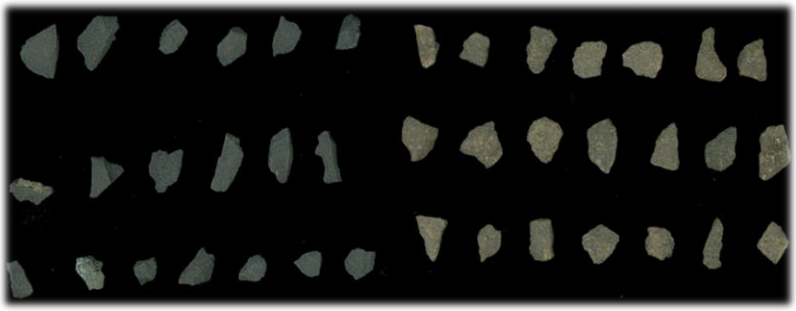

Figure 5: Aggregates samples images after scanning process.

5. Results

Color channels histograms (R, G and B) of weathered and non-weathered aggregates are depicted by the Figures 6, 7 and 8. One can see that there is a difference in the distribution of the color intensity values between the weathered and non-weathered aggregates, mainly in the R channel. For the R channel, the frequency values of the non-weathered aggregates are more concentrated among the histogram bins, indicating that there is a high frequency of some intensity levels. Whereas for the weathered aggregates, the frequency values are more distributed among bins, indicating a smoothing among pixel intensities, very characteristic of the weathering process, which equalizes the natural colors of the minerals. The worst visible distinction in histograms, between weathered and non-weathered aggregates, is observed in B channel. In this case, there is an overlapping of the histogram's bins.

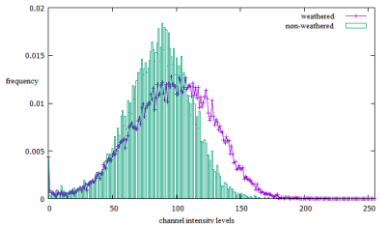

Figure 6: R channel histogram.

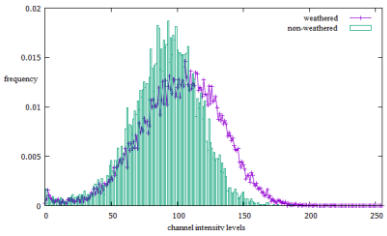

Figure 7: G channel histogram.

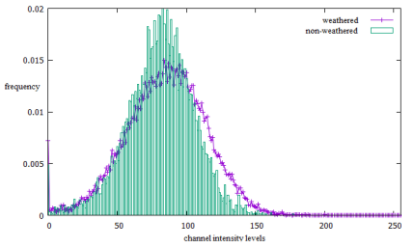

Figure 8: B channel histogram.

The Figures 9, 10 and 11 depict the histograms for the descriptors $LBP_{p,r}$, $LBP_{p,r}^{ri}$ and $LBP_{p,r}^{uni}$, respectively. As there are a large number of bins for the LBPp,r (equal to 256), it was not possible to visually identify significant differences between the histograms for the weathered and non-weathered aggregates. However, differences are noted indicating that in certain tones there is a higher frequency for the weathered aggregate. The $LBP_{p,r}^{ri}$ and $LBP_{p,r}^{uni}$ histograms contain a smaller number of classes, 36 and 60, respectively. For the $LBP_{p,r}^{ri}$ histogram, it was observed that the patterns detected follow a similar distribution, with some binary patterns (classes

of the histogram) with significant difference between weathered and non-weathered aggregates. The same occurred for the $LBP_{p,r}^{uni}$ histogram, in which it can be seen that the last classes accumulate approximately 60% of the frequency values. This fact indicates that the $LBP_{p,r}^{uni}$ algorithm did not obtain a frequency greater than 40% in local and uniform binary patterns in the images.

The Figure 12 illustrates entropy values obtained for each color channel R, G, B, gray and $LPB_{p,r}$. In general, there is no difference among the entropy values obtained for the different channels, except for the R channel. Non-weathered aggregates showed higher entropy values. A possible explanation is that non-weathered aggregates need more information to describe their texture and thus higher entropy values, whereas weathered aggregates by having more uniform shades present lower entropy.

As one can see, some descriptors seem to be able to differentiate the weathered state of the aggregates allowing their classification. Therefore, the next step is to detect the best classification algorithms, using the studied descriptors, so that it is possible to classify the aggregate automatically using machine learning tools.

Machine learning algorithms were used to perform the automatic classification of the aggregates using the Weka software. Histogram values of the aggregates were used as input data for the classification. For entropy, the characteristic vectors were constructed using the entropy values obtained for each RGB component of the digital image.

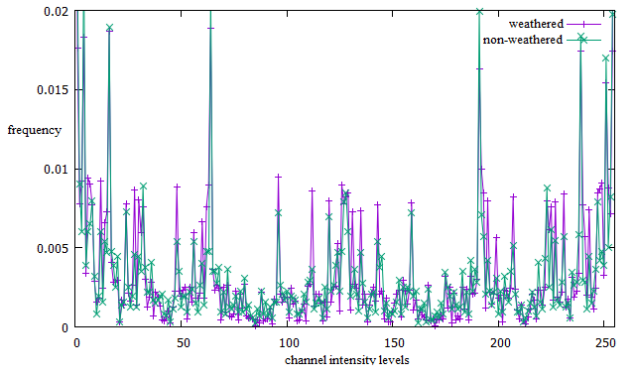

Figure 9: $LBP_{p,r}$ histogram.

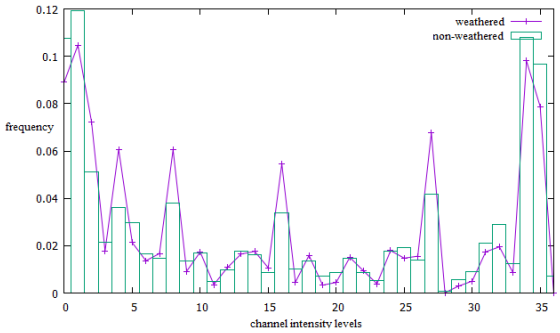

Figure 10: $LBP_{p,r}^{ri}$ histogram.

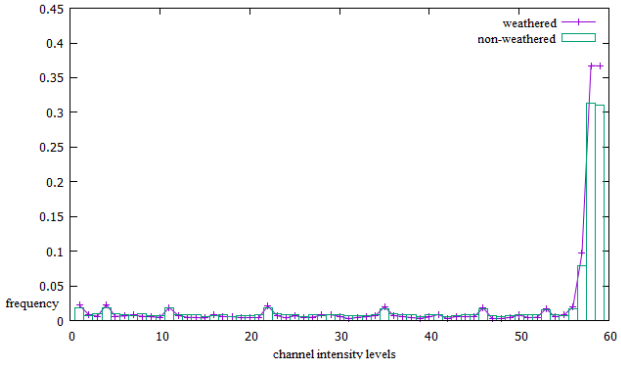

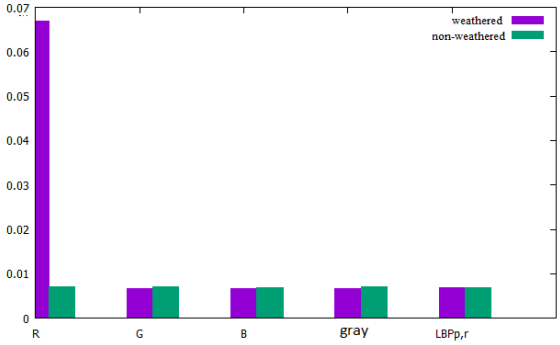

Figure 11: $LBP_{p,r}^{uni}$ histogram.

Figure 12: Entropy values.

As an experimental protocol, cross-validation evaluation with 10 folds was used. In this validation, the data set is divided into 10 subsets of equal size. Then, each subset is used for testing and the rest for training. This step is repeated 10 times and the mean accuracy is registered for each classifier. The accuracies of the classifiers are presented in Table 1.

Table 1: Classifiers accuracy using distinct features vectors.

	Classifier							
	Naive	IBK	IBK	IBK	IBK	IBK	J48	MLP
R histogram	98.23	98.25	97.48	97.77	97.68	97.73	96.16	98.10
G histogram	96.31	96.69	96.20	97.29	96.87	96.84	94.94	97.29
B histogram	88.65	93.46	92.67	93.27	93.35	93.60	93.60	94.44
Gray level histogram	96.55	96.69	96.80	97.46	97.13	95.54	95.54	97.02
$LBP_{p,r}$	85.63	74.51	72.63	77.84	77.77	92.36	92.36	96.29
$LBP^{ri}_{p,b}$	92.67	93.58	94.22	93.80	94.41	94.88	94.88	96.23
$LBPp,r_{uni}$	90.00	93.38	93.91	92.98	93.79	92.87	92.87	95.65
LPQ	83.73	79.88	85.94	80.38	80.98	82.84	82.84	96.72
RGB entropy	83.54	84.75	87.53	86.50	86.58	84.59	84.59	90.75

The results demonstrate that the classifiers obtained better hit rates when the R channel histogram is used as a descriptor. The histogram of channel B produced the worst results when compared with the results using the R, G and gray scale channels.

Among the descriptors based on local binary patterns, the one that produced the best performance was the descriptor $LBP_{p,r}^{ri}$, with an average error around 6% when compared with the $LBP_{p,r}$, and $LBP_{p,r}^{uni}$. This demonstrates that the invariability in relation to rotation allowed to obtain more accurate descriptors in relation to the $LPB_{p,r}$ descriptors. Similarly, this demonstrates that the smaller number of histogram bins when using the $LBP_{p,r}^{uni}$ descriptor was not able to generate descriptors that could distinguish the condition of the aggregates.

When using the entropy and the LPQ algorithm, the classifiers achieved the worst accuracy. The LPQ algorithm produces good results in scenarios where the images are degraded, with low definition or out of focus. As the images were obtained in a controlled environment, the LPQ descriptor did not produce better results than the other descriptors. Regarding entropy, it can be concluded that a single and statistical texture index per sample does not produce good results when compared to the other descriptors.

The classification algorithms were compared using the T test. This method is the one adopted by the Weka software [20] to compare the performance of machine learning algorithms. The accuracy metric was used to compare the performance of the classifiers for each color histogram and descriptors. The results indicate, with a 95% confidence level, that: a) when using

the R channel, the best classifiers was the MLP, IBK and Naive Bayes, which produce statistically equal results and that MLP is better than J48; b) when using the B channel, all classifiers produce statistically equal results, with the exception of the Naive Bayes, which statistically presented a worse classification performance than MLP; c) when using the channel G, all classifiers produced the same classification performance accuracy; d) when using the entropy and the LBP histogram, the MLP performance was better than the others classifiers; e) when using the $LBP_{p,r}^{ri}$, the MLP classifier showed better performance than all classifiers, except for J48, which achieved the same MLP performance; f) when using $LBP_{p,r}^{uni}$, the MLP and IBK classifiers showed the same accuracy and MLP showed better accuracy when compared with the others; g) when using the LPQ descriptor, the MLP classifier showed the better accuracy among all classifiers.

6. Conclusion

Since mineral aggregates are used as the main constituent of many materials used for the purpose of construction works, it must be durable. Durability and soundness are terms typically given to an aggregate's weathering resistance characteristic. Aggregates that are durable are less likely to degrade in the field and cause premature pavement distress.

An assessment of the weathering in a fast and efficient way is very important to improve the quality of the aggregates extracted in quarries. A possible way of using the image analysis is during the aggregate extraction, when images of samples can be collected from the conveyor. This can be useful to control for interrupting the mineral extraction when weathered rocks are detected.

The color histograms, the entropy and the LBP descriptors were evaluated for detecting weathering in basaltic aggregates in order to simplify the existing traditional laboratory tests. The machine learning algorithms demonstrated that color histograms, LBP rotation invariant and LBP uniform descriptors can be promising for this purpose, thus being able to build a machine learning model that can be applied in practice.

7. References

[1] SENGER, L. J.; GOUVEIA, L. T. de. Aplicação de redes neurais ART e análise de textura para a classificação do estado de alteração de agregados minerais. *Revista de Informática Teórica e Aplicada*, v. 17, n. 1, p. 31–51, 2010.
[2] OLIVEIRA, A. M. S.; BRITO., S. N. A. *Geologia de engenharia*. [S.l.], 1998.
[3] MAIA, P. C. A. Avaliação do comportamento geomecânico e de alterabilidade de enrocamentos, Tese, PUC-RJ, 2001.
[4] GIFKINS, W. H. C. C.; LARGE, R. R. Altered volcanic rocks: A guide to description and interpretation. Economic Geology, 2005.
[5] MASAD, E. et al. Test methods for characterizing aggregate shape, texture, and angularity. National Cooperative Highway Research Program – NCHRP, 2005.
[6] WILSON, J.; KLOTZ, L. Quantitative analysis of aggregate based on hough transform. Transportation Research Record, n. 1530, TRB, Washington, DC., 1996.
[7] MASAD, E.; BUTTON, J. W.; PAPAGIANNAKIS, T. Fine aggregate angularity: automated image analysis approach. Transportation Research Record, v.1721, p.66 – 72., 2000.
[8] CHANDAN, C. et al. Application of imaging techniques to geometry analysis of aggregate particles. Journal of Computing in Civil Engineering – ASCE, p. 75 – 82., 2004.
[9] BOWMAN, E. T.; SOGA, K.; DRUMMOND, T. W. Particle shape characterisation using fourier analysis. Relatório técnico, Cambridge University Engineering Department –CUED/D-Soils/TR315, 2000.

[10] GOUVEIA, L. T. de; RODRIGUES, F. A.; COSTA, L. da F. Multiscale Curvature Analysis of Asphaltic Aggregate Particles Journal of Computing in Civil Engineering, v. 24, n. 6, 2010.
[11] SENGER, L. J.; GOUVEIA, L. T. de. Texture analysis of mineral aggregates using entropy. Iberoamerican Journal of Applied Computing, v.1, n.1, 2011.
[12]AHONEN, T.; HADID, A.; PIETIKAINEN, M. Face description with local binary patterns: Application to face recognition. *IEEE Trans. Pattern Analysis and Machine Intelligence*, v. 28, n. 12, p. 2037–2041, 2006.
[13] LIU, L.; FIEGUTH, P. W.; GUO, Y.; WANG, X.; PIETIKAINEN, M. Local binary features for texture classification: Taxonomy and experimental study. Pattern Recognition. V.62., p. 135-160, 2017.
[14] NASIRZADEH, M.; KHAZAEL, A. A.; KHALID, M. b. Woods Recognition System Based on Local Binary Pattern. 2nd International Conference on Computational Intelligence, Communication Systems and Networks, Liverpool, 2010, pp. 308-313.
[15] ZHAO, XURAN; EVANS, NICHOLAS; DUGELAY, JEAN-LUC. A co-training approach to automatic face recognition. EUSIPCO 2011, 19th European Signal Processing Conference. Barcelona, Spain, 2011.
[16] OJALA, T.; PIETIKAINEN, M.; MAENPAA, T. Multiresolution Gray-Scale and Rotation Invariant Texture Classification with Local Binary Patterns. IEEE Transactions on Pattern Analysis and Machine Learning, v. 24, n.7, 2002.
[17] OJANSIVU, V.; RAHTU, E.; HEIKKILä, J. Rotation invariant blur insensitive texture analysis using local phase quantization. Proc. 19th International Conference on Pattern Recognition (ICPR 2008), Tampa, FL, p. 4., 2008.
[18] ALMEIDA, P. R. L. Combinação de características texturais para classificação automática de vagas de estacionamento. *Programa de Pós-Graduação em Informática, UFPR*, 2009.
[19] BRADSKI, G. The OpenCV Library. Dr. Dobb's Journal: Software Tools for the Professional Programmer, v.25 n.11, 2000.
[20] FRANK, E; HALL, M. A.; WITTEN, I. H. The WEKA Workbench. Online Appendix for "Data Mining: Practical Machine Learning Tools and Techniques". Morgan Kaufmann, 4.ed., 2016.